Title

KDM4A Coactivates E2F1 to Regulate the PDK-Dependent Metabolic Switch between Mitochondrial Oxidation and Glycolysis

Journal

Cell Reports, 16(11)

ISSN

2639-1856

Authors

Wang, Ling-Yu
Hung, Chiu-Lien
Chen, Yun-Ru
et al.

Publication Date

2016-09-01

DOI

10.1016/j.celrep.2016.08.018

Peer reviewed

HHS Public Access

Author manuscript

Cell Rep. Author manuscript; available in PMC 2016 September 15.

Published in final edited form as:

Cell Rep. 2016 September 13; 16(11): 3016–3027. doi:10.1016/j.celrep.2016.08.018.

KDM4A coactivates E2F1 to regulate PDK-dependent metabolic switch between mitochondrial oxidation and glycolysis

Ling-Yu Wang[a], **Chiu-Lien Hung**[a,f], **Yun-Ru Chen**[b], **Joy C. Yang**[c], **Junjian Wang**[a], **Mel Campbell**[d], **Yoshihiro Izumiya**[a,d], **Hong-Wu Chen**[a], **Wen-Ching Wang**[e], **David K. Ann**[b], and **Hsing-Jien Kung**[a,f]

[a]Department of Biochemistry and Molecular Medicine, University of California Davis, Sacramento CA 95817, USA

[b]Department of Diabetes Complications and Metabolism, City of Hope, Duarte CA 91010, USA

[c]Department of Urology, University of California Davis, Sacramento CA 95817, USA

[d]Department of Dermatology, University of California Davis, Sacramento CA 95817, USA

[e]Department of Life Sciences, National TsingHua University, Hsinchu 30013, Taiwan

[f]Institute of Molecular and Genomic Medicine, National Health Research Institute, Miaoli 35053, Taiwan

Summary

The histone lysine demethylase KDM4A/JMJD2A has been implicated in prostate carcinogenesis through its role in transcriptional regulation. Here, we describe KDM4A as a E2F1 coactivator and demonstrate a functional role for the E2F1-KDM4A complex in the control of tumor metabolism. KDM4A associates with E2F1 on target gene promoters, enhances E2F1 chromatin binding and transcriptional activity, thereby modulating the transcriptional profile essential for cancer cell proliferation and survival. The pyruvate dehydrogenase kinases PDK1 and PDK3 are direct targets of KDM4A and E2F1, and modulate the switch between glycolytic metabolism and mitochondrial oxidation. Down regulation of KDM4A leads to elevated activity of pyruvate dehydrogenase and mitochondrial oxidation, resulting in excessive accumulation of reactive oxygen species. The altered metabolic phenotypes can be partially rescued by ectopic expression of PDK1 and PDK3, indicating a KDM4A-dependent tumor metabolic regulation via PDK. Our results suggest that KDM4A is a key regulator of tumor metabolism and a potential therapeutic target for prostate cancer.

Corresponding author: Hsing-Jien Kung, PhD, hkung@nhri.org.tw.

Author contributions

L.-Y.W. and H.-J.K. designed research and wrote the paper; L.-Y.W., C.-L.H., Y.-R.C, J.C.Y. and J. W. performed experiments; M.C. edited the paper; Y.I. provided reagents; Y.I., H.-W. C., W.-C.W and D.K.A provided expertise and feedbacks.

We declare no conflict of interests.

Graphical Abstract

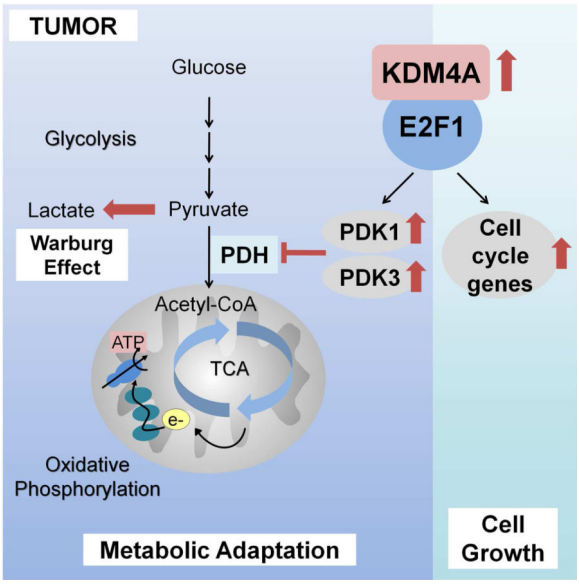

Introduction

Histone lysine methylation is generally involved in transcriptional regulation, and histone lysine demethylase (KDM) is the enzyme that specifically catalyzes the removal of methyl groups from lysine residues. Since discovery of the first KDM, many KDMs have been reported to be genetically altered or aberrantly expressed in a wide spectrum of cancer types (Cloos et al., 2006; Varier and Timmers, 2011). Targeting KDMs thus has been increasingly recognized as an anticancer therapeutic strategy (Hojfeldt et al., 2013; McGrath and Trojer, 2015). KDM4A (or JMJD2A) is Jumonji (JmjC)-domain containing demethylase and belongs to the KDM4 family that specifically demethylates H3K9me3/2 and H3K36me3/2, with the highest affinity towards H3K9me3 (Couture et al., 2007; Hillringhaus et al., 2011; Whetstine et al., 2006). The most characterized role of H3K9me3 is in establishment of heterochromatin; while its existence in euchromatin and active loci represses transcription, is important for gene silencing. Like other KDM4 family members, KDM4A is recognized as a transcriptional regulator for gene activation or repression. When forming complexes with androgen receptor (AR) or estrogen receptor (ER), KDM4A stimulates their transcriptional activity and induces the expression of target genes that are important for proliferation in prostate and breast cancer (Berry et al., 2012; Shin and Janknecht, 2007). On the other hand, KDM4A is also reported as a transcriptional repressor when binding with repressive factors such as nuclear receptor corepressor N-CoR and histone deacetylases (Gray et al., 2005; Zhang et al., 2005). In addition to transcription, KDM4A is also implicated in several other molecular processes such as DNA damage response (Mallette et al., 2012), DNA replication (Black et al., 2010), site-specific copy gain (Black et al., 2013) and translation (Van Rechem et al., 2015). With such diverse roles in cellular processes, it is not surprising that there have been numerous reports about the association of deregulated KDM4A with cancer, including prostate cancers (Chu et al., 2014; Duan et al., 2015; Kim et al., 2016; Shin and Janknecht,

2007). Previously, we reported a small molecule, NSC636819, that exhibits potent inhibition of KDM4A and KDM4B (Chu et al., 2014). We showed that KDM4A and 4B are overexpressed in prostate cancers, and that both pharmacological and genetic inactivation of these KDMs strongly inhibits the cancer growth. Consistently, a recent report identifying another potent inhibitor for KDM4 (Duan et al., 2015) also demonstrated that inhibiting both KDM4A and 4B is a promising therapeutic strategy for castration-resistant prostate cancer (CRPC).

E2F1 is well recognized as a partner of retinoblastoma protein (Rb) and as a critical factor in growth regulation by serving as a transcriptional activator of many cell cycle genes. There is strong evidence that E2F1 is involved in the development of CRPC. For instance, E2F1 overexpression leads to castration-resistance phenotype of LNCaP (Libertini et al., 2006), E2F transcriptome is one of the prominent molecular signatures of CRPC(Sharma et al., 2013), and E2F1 coordinates with AR (Ramos-Montoya et al., 2014) to modulate genes involved in CRPC. In addition to regulating cell cycle and AR genes, E2F1 is also involved in metabolic regulation, as evidenced by the higher oxidative metabolism and lower glycolysis associated with E2F1 homozygous knockout mice (Blanchet et al., 2011). The mechanism however, remains obscure.

Recently, tumor metabolism has gained increasing attention in cancer research. One of cancer cell's hallmarks is the Warburg effect, by which cancer cells heavily rely on glycolysis to obtain energy and produce macromolecules that are required to sustain rapid proliferation. To this end, cancer cells divert the glycolytic metabolite pyruvate from entering mitochondria for the tricarboxylic acid (TCA) cycle, and suppresses oxidative phosphorylation, allowing cancer cells to avoid excessive production of reactive oxygen species (ROS) and prevents mitochondria-driven apoptosis (Cairns et al., 2011; Dang, 2012; Schulze and Harris, 2012). One of the critical gate-keepers controlling the flow of pyruvate to lactate in the cytosol or to acetyl-CoA in mitochondria is pyruvate dehydrogenase kinase (PDK). PDK negatively regulates pyruvate dehydrogenase (PDH), which catalyzes conversion of pyruvate to acetyl-CoA, thereby constraining the utilization of pyruvate for oxidative metabolism while enhancing glycolysis preferred by tumor cells.

In this study, we describe KDM4A as a coactivator of E2F1, and report that KDM4A-E2F complex regulates metabolism by upregulating PDK1 and PDK3, thereby promoting the switch of oxidative phosphorylation to glycolytic metabolism, offering proliferative and survival advantages to prostate cancer cells.

Results

KDM4A addiction by prostate cancer cells *in vitro* and *ex vivo*

Previously, we found that inhibition of KDM4A/4B by the small molecule inhibitor NSC636819, or through knock down by specific shRNA strongly inhibited the growth of LNCaP prostate cancer cells (Chu et al., 2014). Here, we further tested the growth of immortalized normal prostate epithelial cells RWPE-1and two other cancer cell lines, CWR22Rv1 and C4-2B, transduced with control (pLKO.1) or KDM4A knockdown constructs (shKDM4A). The result is consistent with our previous finding showing that

knockdown of KDM4A drastically inhibited proliferation and induced apoptosis in the cancer cells, while no significant differences were observed in the normal RWPE-1 cell (Figure 1A–D). In addition to RWPE-1, we tested PNT2, another immortalized normal prostate epithelial cell, and found no significant effects on proliferation and survival when knocking down KDM4A (Figure S1), suggesting potential addiction to KDM4A evolved in cancer cells. To determine the significance of KDM4A in tumor growth, xenografts were established using control or shKDM4A transduced CWR22Rv1 cells. Similar to *in vitro* cell growth, the xenograft tumor formation and growth derived from KDM4A-knockdown cells was significantly inhibited (Figure 1E). Immunohistochemistry also showed lower expression of the proliferation marker Ki-67 in shKDM4A xenograft tumors (Figure 1F). Together, these results suggest that KDM4A is indispensable for prostate tumor growth *in vitro* and *ex vivo*, and is essential for survival of prostate cancer cells.

KDM4A's association with E2F1 and coregulation of target genes

To understand the mechanism underlying KDM4A-dependent cell growth and survival, the gene expression profiles of KDM4A-knockdown cells was determined by microarray analysis (GEO: GSE77928). A large set of genes involved in cell cycle regulation and cell division were altered in the shKDM4A cells (Figure 2A). Many of these echoed the genes identified in NSC636819 treated cells, including a subset of E2F1 targets (Figure S2A) (Chu et al., 2014). Given that NSC636819 exhibited the strongest inhibitory efficacy towards the KDM4 family compared to other demethylases tested (Figure S2B), the common genes identified upon KDM4A knockdown and inhibitor treatment indicates that KDM4A is likely the major target of NSC636819, and suggests that KDM4A regulates the expression of E2F1 targets. Confirmed by qRT-PCR, down-regulation of the E2F1 target genes appeared to occur in an early response manner 2 days upon KDM4A knockdown, suggesting that they are likely direct transcriptional targets of KDM4A (Figure 2B, S2C). In CWR22Rv1-derived xenografts, the same set of genes were also down-regulated in shKDM4A tumors (Figure 2C), confirming KDM4A-dependent cell cycle gene regulation both *in vitro* and *ex vivo*. To understand whether KDM4A and E2F1 share similar chromatin binding profiles, we surveyed published ChIP-seq datasets for KDM4A (GEO: GSM831035) and E2F1 (GEO: GSM935366), and found an extensive intersection of KDM4A and E2F1 chromatin binding sites (Figure 2D). Although the ChIP-seq analyses were performed using different cell lines for KDM4A and E2F1 (hESC and HeLa, respectively), the overlapped chromatin binding sites strongly suggest that KDM4A and E2F1 share a large set of common targets, and that these two proteins may cooperatively function in transcriptional regulation as a general mechanism across different cell types.

We next determined whether KDM4A and E2F1 physically interact with each other. When co-expressed in 293T cells, HA-tagged E2F1 was co-precipitated with Flag-tagged KDM4A in the anti-Flag immunoprecipitated complex (Figure 3A). Importantly, the interaction of E2F1 and KDM4A was further detected at the endogenous level in both LNCaP and CWR22Rv1 cells, suggesting natural association between these two proteins (Figure 3B). Using various truncates of Flag-KDM4A for co-immunoprecipitation, we mapped the major E2F1 binding domain to aa 249–600 of KDM4A, which covers part of the JmjC domain and its adjacent region (Figure 3C). Reciprocally, in GST pull-down assays using purified GST-

E2F1 fusion proteins and Flag-KDM4A recombinant protein, the KDM4A binding site on E2F1 was mapped to the leucine zipper and marked box dimerization domain (Figure 3D). These results suggest that KDM4A directly associates with E2F1 and coregulates a subset of common target genes.

KDM4A as E2F1 coactivator

We next determined whether KDM4A and E2F1 are co-recruited to the same target loci in prostate cancer cells. ChIP assays with anti-E2F1 and anti-KDM4A antibodies demonstrated that these proteins occupied the same promoter regions of CDC2 and CCNE2 proximal (P) to TSS (Figure 4A). Occupancies at distal regions (D) were used as background controls. The binding of KDM4A-E2F1 complex to target chromatin was further evidenced by ChIP-reChIP assay using anti-KDM4A to pull down the chromatin complex, followed by second precipitation with IgG, anti-E2F1 or anti-KDM4A antibodies (Figure 4B). In addition to CDC2 and CCNE2, the chromatin occupancy of KDM4A was also detected on other E2F1 target promoters such as AURKB, CDC6, CCNE1 and UBE2C (Figure S3A). Interestingly, the chromatin binding of KDM4A and E2F1 on cell cycle genes appeared in a spatial and temporal co-recruitment manner. After release from cell cycle arrest, KDM4A and E2F1 showed similar patterns of chromatin occupancy along cell cycle progression, peaking at S phase in both LNCaP and HeLa cells (Figures 4C, S3B). Using reporter constructs containing the CDC2 or CCNE1 promoter, we next examined whether the presence of KDM4A stimulates E2F1 transcriptional activity. While KDM4A alone did not induce luciferase activity, overexpressing KDM4A with E2F1 strongly enhanced E2F1 transcriptional activity on the target promoters (Figure 4D). Remarkably, this enhancement was not observed when overexpressing catalytic inactive KDM4A(H188A), suggesting that the demethylase activity of KDM4A is required for promoting E2F1 activity (Figure 4D). This requirement was also evidenced by an elevated level of H3K9me3 on the target promoters when knocking down KDM4A, which further led to reduced enrichment of E2F1 and RNA PolII (Figure 4E). Suppressed recruitment of E2F1 by NSC636819 treatment also indicated the importance of demethylase activity (Fig. S3C). While not dramatic, we noted a slight reduction of E2F1 expression after KDM4A knockdown in LNCaP and CWR22Rv1 cells that may also contribute to the lower chromatin binding of E2F1 (Figure S3D). To understand whether E2F1 reciprocally modulates KDM4A recruitment, we knocked down E2F1 and performed KDM4A ChIP assay. Interestingly, the binding of KDM4A was partially inhibited, suggesting that E2F1 also contributes to the targeting and enrichment of KDM4A (Figure S3E). Together, we showed that E2F1 influences the enrichment of KDM4A which in turn, enhances E2F1 binding, and promotes E2F1 transcriptional activity via the histone demethylation activity.

KDM4A regulation of PDKs

Among the altered genes identified in the microarray analysis, downregulation of PDK3 (3 fold) drew our attention because of the increasing appreciation of metabolism in cancer development. PDK regulates the balance of glycolytic and mitochondrial oxidative metabolism through PDH, and plays a critical role in tumor metabolism. In a panel of prostate cells including the primary, immortalized epithelial cells and several cancer cell lines, qRT-PCR showed that PDK1 and PDK3 were generally overexpressed in the cancer

cells; while PDK2 and PDK4 were expressed at significantly lower levels and did not show obvious alteration in cancer cells except for the high PDK4 in CWR22Rv1 cells (Figure S4A). In several clinical datasets, elevated levels of PDK1 and PDK3 are also associated with advanced prostate cancer (Figure S4B), indicating their important roles in the cancer development. Given that PDK4 was previously reported to be a direct target of E2F1 (Hsieh et al., 2008), we asked whether the KDM4A-E2F1 complex also directly regulates transcription of PDK1 and PDK3 in prostate cancer cells. Based on the ENCODE ChIP-seq data, all PDK family members appear to harbor E2F1 binding sites in their promoter regions (Figure 5A;PDK2 and PDK4 not shown). In LNCaP cells, ChIP and ChIP-reChIP assays demonstrated that E2F1 and KDM4A indeed bound to PDK1 and PDK3 promoters in the same complex (Figure 5B, 5C). As expected, when KDM4A was knocked down, the repressive H3K9me3 mark was increased and E2F1 binding was impaired on these promoters (Figure 5D), which is also associated with reduced level of PDK1 and PDK3 expression (Figure 5E). Remarkably, analyses of the expression data from clinical datasets of Sawyers (370 samples), TCGA (497 samples) and Sueltman (95 samples) studies showed a strong positive correlation between KDM4A and PDK1 or PDK3 (Figure S5A). The protein expression in cultured normal and cancerous prostate cells on the other hand, also showed a general positive correlation between KDM4A and the PDKs (Figure S5B). These results together suggest that PDK1 and PDK3 are direct transcriptional targets of KDM4A-E2F1 complex. Consistently, the KDM4A-dependent PDK1 and PDK3 expression was also observed in CWR22Rv1 and C4-2B cells, as well as the CWR22Rv1-derived xenograft tumors (Figure S6A, S6B).

KDM4A-dependent metabolic regulation

After the final step of glycolysis, pyruvate is converted to acetyl-CoA by PDH to fuel the TCA cycle in mitochondria. By directly phosphorylating PDH and inhibiting its activity, PDK tightly modulates the carbon flow from glycolysis into mitochondrial metabolism and cellular respiration. To further determine the biological significance of KDM4A-dependent PDK1 and PDK3 regulation, we examined PDH activity in cells by knocking down KDM4A, PDK1 or PDK3. Phenocopying the PDK-knockdown cells, PDH activity was significantly elevated in KDM4A depleted cells compared to the control group (Figure 6A). The up-regulated PDH activity presumably accelerated the conversion of pyruvate in mitochondria, thereby leading to decreased lactate production and secretion (Figure 6B). These results suggest a shift of glycolytic metabolism to mitochondrial oxidation and respiration via activation of pyruvate dehydrogenase complexes. In agreement with this, the KDM4A-, PDK1-, and PDK3-knockdown cells exhibited significantly lower extracellular acidification rates (ECAR) (Figure 6C) and higher oxygen consumption rates (OCR) at both basal and maximal levels, coupled with increased ATP synthesis capacity (Figure 6D), indicating reduced acidification from glycolysis and elevated mitochondrial oxidative phosphorylation. As a consequence of enhanced respiration, these cells displayed excessive ROS production in the mitochondria, labeled by MitoSOX (Figure 6E). Consistent with the effects observed in LNCaP, KDM4A knockdown in CWR22Rv1 cell also increased the cellular PDH activity and mitochondrial ROS accumulation (Figure S6C, S6D). Moreover, pharmacological inhibition of KDM4A by NSC636819 treatment also led to similar metabolic phenotypes (Figure S7A–G). These data collectively showed that KDM4A plays

an important role in modulating the cellular metabolic switch between glycolysis and oxidative phosphorylation by controlling PDK1 and PDK3 expression. Given that knocking down these PDKs strongly inhibited cell proliferation (Figure 6F) and induced caspase 3/7 activation (Figure 6G), we suggest that the KDM4A-dependent PDK1 and PDK3 expression and their high levels in prostate cancer cell play a critical role in tumor growth and survival.

To confirm that the KDM4A-mediated metabolic regulation is indeed channeled through PDK1 and PDK3, we ectopically expressed these kinases in the KDM4A-knockdown cell by lentiviral transduction. Compared to the empty vector control, expression of PDK1 and PDK3 is able to rescue the shKDM4A-induced metabolic defects partially, but with statistical significance. The rescued phenotypes included lower PDH activity, higher glycolysis and lactate production, and decreased oxygen consumption rates (Figure 7A–D). The accumulation of total and mitochondrial ROS in shKDM4A cells was also reduced when overexpressing PDK1 or PDK3 (Figure 7F). This restoration suggests that PDK1 and PDK3 are the effectors of KDM4A in modulating the glycolytic and oxidative metabolism.

Discussion

KDM4A is overexpressed in many cancer types including prostate, breast, lung and colon cancers and its expression is critical for cell proliferation (Berry et al., 2012; Chu et al., 2014; Cloos et al., 2006; Kim et al., 2012; Li et al., 2012; Li et al., 2011; Mallette and Richard, 2012). We previously reported that by selectively inhibiting KDM4A/4B with a small molecule inhibitor, the LNCaP prostate cancer cells displayed drastic growth retardation and increased apoptosis (Chu et al., 2014). Here, we showed that knockdown of KDM4A with specific shRNAs inhibited cell growth and induced apoptosis in prostate cancer cells, but not in immortalized prostate epithelial cells. These results suggest that the cancer cells may have evolved addiction to higher level and pro-tumor properties of KDM4A. Significantly, downregulation of KDM4A impaired tumor formation in CWR22Rv1 xenografts. Given that progression of prostate cancer into CRPC remains the biggest challenge for intervention, our finding of the effective growth inhibition and cell death induction achieved by KDM4A knockdown in the castration resistant CWR22Rv1 and C4-2B cells, provides supportive evidence for KDM4A as a potential therapeutic target in advanced prostate cancer.

KDM4A was first implicated in prostate cancer with its function in AR signaling pathway (Shin and Janknecht, 2007). A recent report showed that KDM4A drives prostate cancer development via transcription factor EVT1 and the downstream target YAP1 expression (Kim et al., 2016). Here, we report that E2F1 is another transcriptional factor regulated by KDM4A, and demonstrate an E2F1-KDM4A functional connection in the control of tumor growth. First, expression of a subset of E2F1 targets involved in cell cycle, DNA replication, chromosome organization and chromosome segregation was significantly altered in KDM4A-knockdown cells and in a xenograft model. Second, KDM4A physically interacts with E2F1. Third, KDM4A and E2F1 are co-recruited to the same targets and share significantly overlapped chromatin binding sites. Fourth, overexpression of KDM4A enhances E2F1 transcriptional activity in a demethylase activity-dependent manner. Finally, knockdown of KDM4A results in elevated H3K9me3 and decreased occupancy of E2F1 on

the target promoters. Reciprocally, E2F1 depletion influences the enrichment of KDM4A on targets, indicating that E2F1 can help KDM4A's target recognition and occupancy. The binding of KDM4A in turn, alters the local chromatin status and further enhances E2F1 binding. Our data not only provides mechanistic evidence for KDM4A-dependent gene regulation through E2F1, but also echoes the finding of Black *et al.* that shows by regulating the level of H3K9me3 and subsequently attenuating chromatin binding for heterochromatin protein 1 gamma, overexpression of KDM4A increases chromatin accessibility for DNA replication machinery and facilitates S phase progression (Black et al., 2010). The involvement of KDM4A in cell cycle regulation is also supported by its counteracting partner, Suv39H1 methyltransferase, which dissociates from chromatin during S to G2-M transitions, thereby promoting the KDM4A occupancy (Park et al., 2014). Our results support the notion that concerted activities from multiple histone modifiers regulate the balance of active and repressive histone marks on E2F-responsive promoters to fine-tune gene expression and coordinate cell cycle transition.

In addition to its function in cell cycle, we describe a role of KDM4A-E2F1 in tumor metabolism. This resonates with a recent report (Zhao et al., 2016), which links KDM4C to amino acid metabolism. We found KDM4A-E2F1 is involved in glycolytic and oxidative metabolic regulation by increasing PDK expression. As a gate-keeping enzyme for conversion of pyruvate into acetyl-CoA in mitochondria, PDK plays a pivotal role in shifting cell metabolism towards glycolysis to support the proliferative and survival needs of tumor cells. Because of this distinct feature in cancer, targeting PDK has been recognized as an effective anticancer therapeutic strategy. Numerous pre-clinical studies showed that a small molecule inhibitor of PDK, dichloroacetate (DCA), is effective in inhibiting proliferation of a wide range of cancers by reversing the glycolytic phenotype, depolarizing mitochondria, and inducing apoptosis (Bhat et al., 2015; Sutendra and Michelakis, 2013). Here, we provide evidence showing that PDK1 and PDK3 are overexpressed in prostate cancer cells, and that their overexpression is associated with advanced cancers. Likewise, knockdown of these PDKs drastically inhibited proliferation and induced apoptosis with severe oxidative phenotypes in prostate cancer cells. We showed that KDM4A induces transcription of PDK1 and PDK3 by altering the chromatin status, thus enhancing E2F1 transcriptional activity on these genes. Downregulation of the PDKs by KDM4A inhibition shifted the metabolism towards oxidative phosphorylation and caused excessive accumulation of ROS that may contribute to the induction of apoptosis. Moreover, ectopic expression of PDK1 or PDK3 partially rescued the shKDM4A-induced metabolic phenotypes, demonstrating that the KDM4A-dependent metabolic regulation is at least in part channeled through PDK1 and PDK3. The reasons that we do not see full rescue could be due to two possibilities. First, KDM4A may participate in the modulation of other cellular factors involved in metabolic regulation. Second, overexpressing PDK1 and PDK3 individually may not achieve the combined level of all four members. Several pieces of evidence indicate that dysregulation of PDK in cancer is contributed by oncogenes and tumor suppressors such as HIF1α, c-Myc, p53 and Rb. (Contractor and Harris, 2012; Hsieh et al., 2008; Kim et al., 2007; Papandreou et al., 2006). Together with our findings, the evidence collectively suggests that tumor cells utilize multiple pathways including epigenetic modification to ensure the activation of pyruvate dehydrogenase complex during cancer progression.

Cell proliferation requires coordination between metabolic signals and cell cycle machinery. Although the mechanism is not fully understood, increasing evidence indicates that cell cycle regulators such as E2F1, Rb, Cdk4, and cyclin D possess dual roles in both cell cycle and metabolic control (Fajas, 2013). The cooperative role of KDM4A and E2F1 described in this study provides the first evidence of an epigenetic link for cell cycle and metabolic regulation.

Although KDM4A was reported to suppress gene expression (Gray et al., 2005; Zhang et al., 2005), we found that KDM4A plays primarily an activating role for E2F1, as did several other reports, which documented KDM4A as an activator (Berry et al., 2012; Shin and Janknecht, 2007). It seems that KDM4A's role in repression or activation depends on its binding partners as well as the requirement for demethylation activities. While it is not clear whether KDM4A-mediated repression requires its demethylase activity, our work as well as that of others (Berry et al., 2012; Shin and Janknecht, 2007) all indicate the importance of H3K9me3 removal in the activation. Further study will be needed to understand how KDM4A coordinates both activation and repression on E2F1 targets. As an enzyme, KDM4A offers itself as a potentially “druggable” target for tumor metabolic reprogramming. Given that some cancer cells lack the expression of DCA transporter SLC5A8 and hence require higher doses of DCA to achieve antitumor effects (Babu et al., 2011), KDM4A may serve as an effective alternative for metabolic targeting.

In summary, we uncovered a KDM4A-E2F1 connection and described KDM4A-dependent transcriptional regulation of PDK1 and PDK3 in promoting tumor glycolytic switch in prostate cancer cells. This finding sheds light on the role of epigenetic regulators in tumor metabolism that may be exploited therapeutically.

Experimental procedures

Cell culture

RWPE-1, LNCaP, CWR22Rv1, PC3, and HEK293Tcells were purchased from ATCC and cultured according to instructions provided. LNCaP derived C4-2 cells (Thalmann et al., 1994) were cultured in RPMI1640 medium supplemented with 10% FBS. Synchronization of LNCaP cells at the G1/S was induced by double-thymidine block: thymidine (2 mM) treatment for 18hr, washed and released in complete medium for 9hr, followed by 16hr of thymidine (2 mM) treatment.

Plasmids and reagents

pLKO.1-shKDM4A(clone ID: TRCN0000013493, TRCN0000234910), pLKO.1-shPDK1 (TRCN0000006261) and pLKO.1-shPDK3 (TRCN0000379916) plasmids were obtained from TRC library. pDONR223-PDK1 (Addgene plasmid # 23804) and pDONR223-PDK3 (Addgene plasmid # 23556) were gifts from William Hahn & David Root distributed by Addgene. The PDK1 and PDK3 cDNAs were amplified and cloned into pLenti4 vector (Invitrogen) modified with insertion of a CpoI cloning site. All lentivirus was produced as described in (Chu et al., 2014). HA-E2F1, CDC2-luciferase and CCNE1-luciferase plasmids are as described in (Revenko et al., 2010). KDM4A was cloned into pcDNA3-Flag vector

and recombinant baculovirus transfer vector pFAST-BAC (Invitrogen). The full-length and various truncated E2F1 were cloned into pGEX vector for GST-fusion protein construction.

Cell proliferation and caspase activity

Cell proliferation was measured and detected by MTT Cell Proliferation Kit I (Roche) and crystal violet staining. Cells were seeded in triplicate in 48-well plates 1 day prior to lentivirus infection (day 0), followed by the MTT assay performed on days 0, 2, 4, 6, and 8 according to manufacturer's instructions. 50,000 cells were seeded in 12-well plates 1 day before lentivirus infection. 8 days after infection, the cells were fixed by methanol and stained by 0.5% crystal violet to visualize the cell expansion. Cellular caspase activity was measured by Caspase-Glo 3/7 assay system (Promega) according the manufacturer's instructions.

Xenograft

CWR22Rv1 cells were infected by pLKO.1 or shKDM4A lentivirus for 48 hr. 3 million infected cells were implanted subcutaneously into 10 nude mice for each group. 10 days after implantation, the tumor volume was measured every 2–3 days for 3 weeks. The tumor tissues were harvested and immediately frozen in liquid nitrogen for RNA isolation; or fixed in formalin for paraffin block preparation. The animal study was performed according to the protocols approved by the Institutional Animal Care and Use Committee of the UC Davis. The formalin-fixed tissues were processed in UC Davis Cancer Center Biorepository Core for paraffin embedding, sectioning and IHC staining. Anti-JMJD2A (NeuroMab) antibody was used for KDM4A IHC staining.

Quantitative PCR

RNeasy plus kits (Qiagen) were used to isolate total RNA. cDNA was synthesized using SuperScript III first-strand synthesis reagents (Invitrogen). The amount of cDNA was then quantified by the Bio-Rad CFX Real-Time PCR detection system using SYBR Green Super mix (Fermentas) and primers listed in Table S1. All samples were tested in triplicate, and the expression levels were normalized against actin mRNA, GAPDH mRNA, and 18S ribosomal RNA.

Immunoprecipitation and western blotting

To obtain total lysates, cells were lysed in RIPA buffer (50 mM Tris pH8.0, 150 mM NaCl, 1% NP-40, 0.5% Na-deoxycholate, 0.5% SDS, protease inhibitors) on ice, followed by 10 min of sonication by Bioruptor. For IP, cells were lysed with buffer containing Tris-HCl (50 mM, pH8.0), NaCl (150 mM), Triton X-100 (0.5%), glycerol (10%), EDTA (1 mM) and protease inhibitors for 15 min on ice. The lysates were then incubated with Flag-M2 agarose (Sigma-Aldrich) or anti-JMJD2A (NeuroMab) at 4°C overnight. The precipitated protein complexes were washed four times next day. Proteins were resolved in SDS-PAGE for western blotting. Western blot images were taken by FluorChem E system and analyzed by AlphaView SA software. Antibodies used include: KDM4A (NeuroMab), Flag-M2 and β-actin (Sigma-Aldrich), HA (Covance), cyclin B1 and E2F1 (Santa Cruz), p-H3S10

(Millipore), PDK1 and PDK3 (Abcam). GST antibody was purified from rabbit antiserum generated against a GST-tagged antigen.

Recombinant protein purification and GST pull down assay

GST, GST-E2F1 truncated proteins were expressed in *E. coli* strain BL21. The bacteria was lysed by standard procedure, followed by incubation with Glutathione-Sepharose beads (Pharmacia), washes and elution in 50 mM Tris–HCl pH8.0, 400 mM NaCl, 1 mM dithiothreitol, 1% Triton X-100, 20 mM glutathione. Flag tagged KDM4A was purified from recombinant baculovirus infected Sf9 cells with the procedure described previously (Izumiya et al., 2007). The purified recombinant GST-E2F1 and Flag-KDM4A proteins were incubated at 4°Cfor 4hr, followed by washes and western blotting analysis.

ChIP and ChIP-reChIP

ChIP was performed following the UC Davis Genome Center ChIP protocol. Briefly, cells were crosslinked by formaldehyde (1%). The crosslinked chromatin was sonicated to fragment DNA to 200–500bp. The lysate was pre-cleared by protein A/G agarose and subsequently incubated with specific antibodies: mouse IgG (Millipore), KDM4A (Bethyl), E2F1 (Millipore), H3 and H3K9me3 (Abcam), PolII (Genetex) for overnight at 4°C. The ChIP complexes were washed and eluted in 50 mM NaHCO3 and 1% SDS, followed by overnight reverse crosslinking. For reChIP, KDM4A bound chromatin was eluted in buffer containing 50 mM NaHCO3, 1% SDS, 10 mM DTT. The eluted ChIP complex was diluted 40× with ChIP IP buffer and incubated with IgG, anti-E2F1 or anti-KDM4A overnight at 4°C for second time ChIP. The recovered DNAs from ChIP and ChIP-reChIP were analyzed by qPCR using the primers listed in Table S2. For the published ChIP-seq datasets analysis, the BED files of H1 hESCs-JMJD2A ChIP-seq (GSM831035) and HeLa-S3_HA-E2F1_std ChIP-seq (GSM935366) were downloaded. Overlapping peaks in each BED were merged using the BEDTools 'merge' command. In the JMJD2A dataset, 21,418 peaks were merged into 18,033 peaks, and in the E2F1 dataset the number of peaks remained unchanged (5,153). The merged BEDs were then intersected with each other using the BEDTools 'intersect' command.

Luciferase assay

PC3 cells were seeded in 24-well plates 1 day prior to transfection. Cells were co-transfected with empty Flag vector, Flag-KDM4A or Flag-KDM4A(H188A) with HA or HA-E2F1, together with CDC2-luc or CCNE1-luc plasmid. pRL-SV40 Renilla luciferase plasmid was used as transfection control. The luciferase activity was detected using Dual-luciferase Assay Kit (Promega). All samples were tested in triplicate and the luciferase relative light units (RLU) were normalized against the Renilla values.

Microarray

Global expression analysis was performed in LNCaP cells transduced with shKDM4A or pLKO.1 for 3 days (GEO accession GSE77928). Microarray analysis was performed by the UC Davis Comprehensive Cancer Center Gene Expression Resource, using Affymetrix Human Genome U133A Gene Chip arrays, which permits expression analysis of the entire

Genbank RefSeq database. Subsequent data analysis was done by Gene Spring (Agilent Technologies) and DAVID bioinformatic resources.

Metabolic assays and mitochondrial ROS detection

Cell culture media and cell pellets were harvested 3 days after lentiviral delivery of pLKO.1 or knockdown constructs. The cellular PDH activity and lactate concentration in cultured media was measured using commercial kits (BioVision Inc.) following the manufacture's instructions. All samples were tested in triplicate. Mitochondrial superoxide was detected by MitoSOX fluorescent indicator (Invitrogen). Briefly, cells were seeded on cover glass in 6-well plates before subjected to lentivirus infection. 4 days after transduction, cells were washed with PBS and HBSS, followed by incubation with MitoSOX (2.5 μM) for 30 min at 37°C in dark. The stained cells were washed, paraformaldehyde fixed, permeabilized and stained with DAPI to label nuclei. The cells were visualized by confocal fluorescence microscopy (Zeiss LSM710). In each experiment, images of equal stacks of confocal sections were taken, and random fields of view were selected. The Z-section images were processed by maximal projection using Image J. Cellular ROS was labeled by 2′,7′-dichlorodihydrofluorescein diacetate (CM-H2DCFDA, Invitrogen) following the procedure described in (Eruslanov and Kusmartsev, 2010). Briefly, equal amount of cells were labeled with CM-H2DCFDA (10 μM) for 45 min and washed by HBSS. The fluorescent signal was detected at Ex/Em = 485/535 nm.

Oxygen consumption and extracellular acidification rate

Cellular mitochondrial function was determined using the Seahorse Bioscience XF24 Extracellular Flux analyzer according to manufacturer's instructions. Cells were seeded in Seahorse plates and incubated overnight before infection by lentivirus carrying pLKO.1 or knockdown constructs for 3 days. XF Cell Mito Stress and Glycolysis Stress test kits were used following the manufacturer’s protocol.

Statistical Analysis

Experiments were performed in triplicate. Statistical analysis of the differences between two groups was determined by two-tailed Student’s t test. p values less than 0.05 were considered to be significant.

Supplementary Material

Refer to Web version on PubMed Central for supplementary material.

Acknowledgments

This work was supported by US National Institutes of Health Grants CA114575, CA165263, R01DE10742 and P30CA33573. We also acknowledge grants supported by National Health Research Institutes of Taiwan (03A1-MGPP18-014). We are grateful to Ryan R. Davis (UCDCCC Genomics Shared Resource) for his expert technical assistance for the microarray studies, and Joseph Fass (UC Davis Genome Center Bioinformatics Core) for his expert analysis of the published ChIP-seq data.

References

Babu E, Ramachandran S, CoothanKandaswamy V, Elangovan S, Prasad PD, Ganapathy V, Thangaraju M. Role of SLC5A8, a plasma membrane transporter and a tumor suppressor, in the antitumor activity of dichloroacetate. Oncogene. 2011; 30:4026–4037. [PubMed: 21499304]

Berry WL, Shin S, Lightfoot SA, Janknecht R. Oncogenic features of the JMJD2A histone demethylase in breast cancer. International journal of oncology. 2012; 41:1701–1706. [PubMed: 22948256]

Bhat TA, Kumar S, Chaudhary AK, Yadav N, Chandra D. Restoration of mitochondria function as a target for cancer therapy. Drug discovery today. 2015; 20:635–643. [PubMed: 25766095]

Black JC, Allen A, Van Rechem C, Forbes E, Longworth M, Tschop K, Rinehart C, Quiton J, Walsh R, Smallwood A, et al. Conserved antagonism between JMJD2A/KDM4A and HP1gamma during cell cycle progression. Molecular cell. 2010; 40:736–748. [PubMed: 21145482]

Black JC, Manning AL, Van Rechem C, Kim J, Ladd B, Cho J, Pineda CM, Murphy N, Daniels DL, Montagna C, et al. KDM4A lysine demethylase induces site-specific copy gain and rereplication of regions amplified in tumors. Cell. 2013; 154:541–555. [PubMed: 23871696]

Blanchet E, Annicotte JS, Lagarrigue S, Aguilar V, Clape C, Chavey C, Fritz V, Casas F, Apparailly F, Auwerx J, et al. E2F transcription factor-1 regulates oxidative metabolism. Nature cell biology. 2011; 13:1146–1152. [PubMed: 21841792]

Cairns RA, Harris IS, Mak TW. Regulation of cancer cell metabolism. Nature reviews Cancer. 2011; 11:85–95. [PubMed: 21258394]

Chu CH, Wang LY, Hsu KC, Chen CC, Cheng HH, Wang SM, Wu CM, Chen TJ, Li LT, Liu R, et al. KDM4B as a target for prostate cancer: structural analysis and selective inhibition by a novel inhibitor. Journal of medicinal chemistry. 2014; 57:5975–5985. [PubMed: 24971742]

Cloos PA, Christensen J, Agger K, Maiolica A, Rappsilber J, Antal T, Hansen KH, Helin K. The putative oncogene GASC1 demethylates tri- and dimethylated lysine 9 on histone H3. Nature. 2006; 442:307–311. [PubMed: 16732293]

Contractor T, Harris CR. p53 negatively regulates transcription of the pyruvate dehydrogenase kinase Pdk2. Cancer research. 2012; 72:560–567. [PubMed: 22123926]

Couture JF, Collazo E, Ortiz-Tello PA, Brunzelle JS, Trievel RC. Specificity and mechanism of JMJD2A, a trimethyllysine-specific histone demethylase. Nature structural & molecular biology. 2007; 14:689–695.

Dang CV. Links between metabolism and cancer. Genes & development. 2012; 26:877–890. [PubMed: 22549953]

Duan L, Rai G, Roggero C, Zhang QJ, Wei Q, Ma SH, Zhou Y, Santoyo J, Martinez ED, Xiao G, et al. KDM4/JMJD2 Histone Demethylase Inhibitors Block Prostate Tumor Growth by Suppressing the Expression of AR and BMYB-Regulated Genes. Chemistry & biology. 2015; 22:1185–1196. [PubMed: 26364928]

Eruslanov E, Kusmartsev S. Identification of ROS using oxidized DCFDA and flow-cytometry. Methods in molecular biology. 2010; 594:57–72. [PubMed: 20072909]

Fajas L. Re-thinking cell cycle regulators: the cross-talk with metabolism. Frontiers in oncology. 2013; 3:4. [PubMed: 23355973]

Gray SG, Iglesias AH, Lizcano F, Villanueva R, Camelo S, Jingu H, Teh BT, Koibuchi N, Chin WW, Kokkotou E, et al. Functional characterization of JMJD2A, a histone deacetylase- and retinoblastoma-binding protein. The Journal of biological chemistry. 2005; 280:28507–28518. [PubMed: 15927959]

Hillringhaus L, Yue WW, Rose NR, Ng SS, Gileadi C, Loenarz C, Bello SH, Bray JE, Schofield CJ, Oppermann U. Structural and evolutionary basis for the dual substrate selectivity of human KDM4 histone demethylase family. The Journal of biological chemistry. 2011; 286:41616–41625. [PubMed: 21914792]

Hojfeldt JW, Agger K, Helin K. Histone lysine demethylases as targets for anticancer therapy. Nature reviews Drug discovery. 2013; 12:917–930. [PubMed: 24232376]

Hsieh MC, Das D, Sambandam N, Zhang MQ, Nahle Z. Regulation of the PDK4 isozyme by the Rb-E2F1 complex. The Journal of biological chemistry. 2008; 283:27410–27417. [PubMed: 18667418]

Izumiya Y, Izumiya C, Van Geelen A, Wang DH, Lam KS, Luciw PA, Kung HJ. Kaposi's sarcoma-associated herpesvirus-encoded protein kinase and its interaction with K-bZIP. Journal of virology. 2007; 81:1072–1082. [PubMed: 17108053]

Kim JW, Gao P, Liu YC, Semenza GL, Dang CV. Hypoxia-inducible factor 1 and dysregulated c-Myc cooperatively induce vascular endothelial growth factor and metabolic switches hexokinase 2 and pyruvate dehydrogenase kinase 1. Molecular and cellular biology. 2007; 27:7381–7393. [PubMed: 17785433]

Kim TD, Jin F, Shin S, Oh S, Lightfoot SA, Grande JP, Johnson AJ, van Deursen JM, Wren JD, Janknecht R. Histone demethylase JMJD2A drives prostate tumorigenesis through transcription factor ETV1. The Journal of clinical investigation. 2016; 126:706–720. [PubMed: 26731476]

Kim TD, Shin S, Berry WL, Oh S, Janknecht R. The JMJD2A demethylase regulates apoptosis and proliferation in colon cancer cells. Journal of cellular biochemistry. 2012; 113:1368–1376. [PubMed: 22134899]

Li BX, Luo CL, Li H, Yang P, Zhang MC, Xu HM, Xu HF, Shen YW, Xue AM, Zhao ZQ. Effects of siRNA-mediated knockdown of jumonji domain containing 2A on proliferation, migration and invasion of the human breast cancer cell line MCF-7. Experimental and therapeutic medicine. 2012; 4:755–761. [PubMed: 23170139]

Li BX, Zhang MC, Luo CL, Yang P, Li H, Xu HM, Xu HF, Shen YW, Xue AM, Zhao ZQ. Effects of RNA interference-mediated gene silencing of JMJD2A on human breast cancer cell line MDA-MB-231 in vitro. Journal of experimental & clinical cancer research : CR. 2011; 30:90. [PubMed: 21962223]

Libertini SJ, Tepper CG, Guadalupe M, Lu Y, Asmuth DM, Mudryj M. E2F1 expression in LNCaP prostate cancer cells deregulates androgen dependent growth, suppresses differentiation, and enhances apoptosis. The Prostate. 2006; 66:70–81. [PubMed: 16114066]

Mallette FA, Mattiroli F, Cui G, Young LC, Hendzel MJ, Mer G, Sixma TK, Richard S. RNF8- and RNF168-dependent degradation of KDM4A/JMJD2A triggers 53BP1 recruitment to DNA damage sites. The EMBO journal. 2012; 31:1865–1878. [PubMed: 22373579]

Mallette FA, Richard S. JMJD2A promotes cellular transformation by blocking cellular senescence through transcriptional repression of the tumor suppressor CHD5. Cell reports. 2012; 2:1233–1243. [PubMed: 23168260]

McGrath J, Trojer P. Targeting histone lysine methylation in cancer. Pharmacology & therapeutics. 2015; 150:1–22. [PubMed: 25578037]

Papandreou I, Cairns RA, Fontana L, Lim AL, Denko NC. HIF-1 mediates adaptation to hypoxia by actively downregulating mitochondrial oxygen consumption. Cell metabolism. 2006; 3:187–197. [PubMed: 16517406]

Park SH, Yu SE, Chai YG, Jang YK. CDK2-dependent phosphorylation of Suv39H1 is involved in control of heterochromatin replication during cell cycle progression. Nucleic acids research. 2014; 42:6196–6207. [PubMed: 24728993]

Ramos-Montoya A, Lamb AD, Russell R, Carroll T, Jurmeister S, Galeano-Dalmau N, Massie CE, Boren J, Bon H, Theodorou V, et al. HES6 drives a critical AR transcriptional programme to induce castration-resistant prostate cancer through activation of an E2F1-mediated cell cycle network. EMBO molecular medicine. 2014; 6:651–661. [PubMed: 24737870]

Revenko AS, Kalashnikova EV, Gemo AT, Zou JX, Chen HW. Chromatin loading of E2F-MLL complex by cancer-associated coregulator ANCCA via reading a specific histone mark. Molecular and cellular biology. 2010; 30:5260–5272. [PubMed: 20855524]

Schulze A, Harris AL. How cancer metabolism is tuned for proliferation and vulnerable to disruption. Nature. 2012; 491:364–373. [PubMed: 23151579]

Sharma NL, Massie CE, Ramos-Montoya A, Zecchini V, Scott HE, Lamb AD, MacArthur S, Stark R, Warren AY, Mills IG, et al. The androgen receptor induces a distinct transcriptional program in castration-resistant prostate cancer in man. Cancer cell. 2013; 23:35–47. [PubMed: 23260764]

Shin S, Janknecht R. Activation of androgen receptor by histone demethylases JMJD2A and JMJD2D. Biochemical and biophysical research communications. 2007; 359:742–746. [PubMed: 17555712]

Sutendra G, Michelakis ED. Pyruvate dehydrogenase kinase as a novel therapeutic target in oncology. Frontiers in oncology. 2013; 3:38. [PubMed: 23471124]

Thalmann GN, Anezinis PE, Chang SM, Zhau HE, Kim EE, Hopwood VL, Pathak S, von Eschenbach AC, Chung LW. Androgen-independent cancer progression and bone metastasis in the LNCaP model of human prostate cancer. Cancer research. 1994; 54:2577–2581. [PubMed: 8168083]

Van Rechem C, Black JC, Boukhali M, Aryee MJ, Graslund S, Haas W, Benes CH, Whetstine JR. Lysine demethylase KDM4A associates with translation machinery and regulates protein synthesis. Cancer discovery. 2015; 5:255–263. [PubMed: 25564516]

Varier RA, Timmers HT. Histone lysine methylation and demethylation pathways in cancer. Biochimica et biophysica acta. 2011; 1815:75–89. [PubMed: 20951770]

Whetstine JR, Nottke A, Lan F, Huarte M, Smolikov S, Chen Z, Spooner E, Li E, Zhang G, Colaiacovo M, et al. Reversal of histone lysine trimethylation by the JMJD2 family of histone demethylases. Cell. 2006; 125:467–481. [PubMed: 16603238]

Zhang D, Yoon HG, Wong J. JMJD2A is a novel N-CoR-interacting protein and is involved in repression of the human transcription factor achaete scute-like homologue 2 (ASCL2/Hash2). Molecular and cellular biology. 2005; 25:6404–6414. [PubMed: 16024779]

Zhao E, Ding J, Xia Y, Liu M, Ye B, Choi JH, Yan C, Dong Z, Huang S, Zha Y, et al. KDM4C and ATF4 Cooperate in Transcriptional Control of Amino Acid Metabolism. Cell reports. 2016; 14:506–519. [PubMed: 26774480]

Highlights

- KDM4A is a coactivator of E2F1 and promotes tumor growth
- KDM4A-E2F1 complex regulates cell cycle and tumor metabolism
- KDM4A recruits E2F1 for efficient transcriptional activation of PDK
- Targeting KDM4A reverses glycolytic metabolism to mitochondrial oxidation

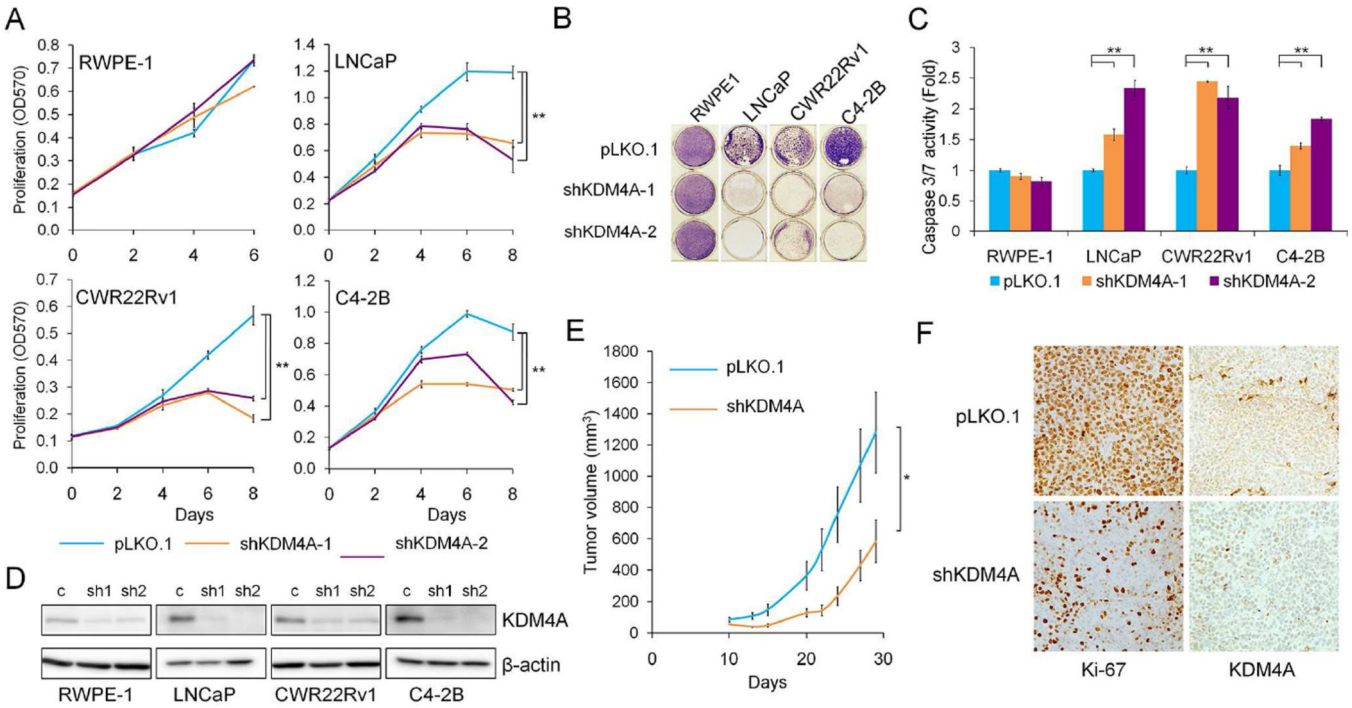

Figure 1.

KDM4A is essential for tumor cell proliferation. (A) MTT cell proliferation assay and (B) crystal violet staining of normal immortalized RWPE-1 cell and prostate cancer cell lines LNCaP, CWR22Rv1 and C4-2B, infected with lentivirus carrying control pLKO.1 or shKDM4A constructs. The cells were infected on day 0, and MTT was added to detect viable cells every two days after infection. 8 days after lentiviral infection, the cells were fixed and stained by crystal violet. (C) Caspase 3/7 activity of the lentiviral-infected cells was detected on day 6. (D) 3 days after infection, the expression of KDM4A was examined by western blotting. (E) CWR22Rv1 xenograft tumor growth. CWR22Rv1 cells were infected by lentivirus carrying pLKO.1 or shKDM4A for 2 days, and then implanted subcutaneously into nude mice. 10 days after implantation, the tumor volumes were measured up to 3 weeks. Data are presented as mean ± SD, with the SD derived from 10 mice. (F) Ki-67 and KDM4A immunohistochemistry staining of the tumor sections isolated from the xenografts. All cell culture-based data are presented as the average of n ≥ 3 replicates ± SD. **:p< 0.01, *: p<0.05

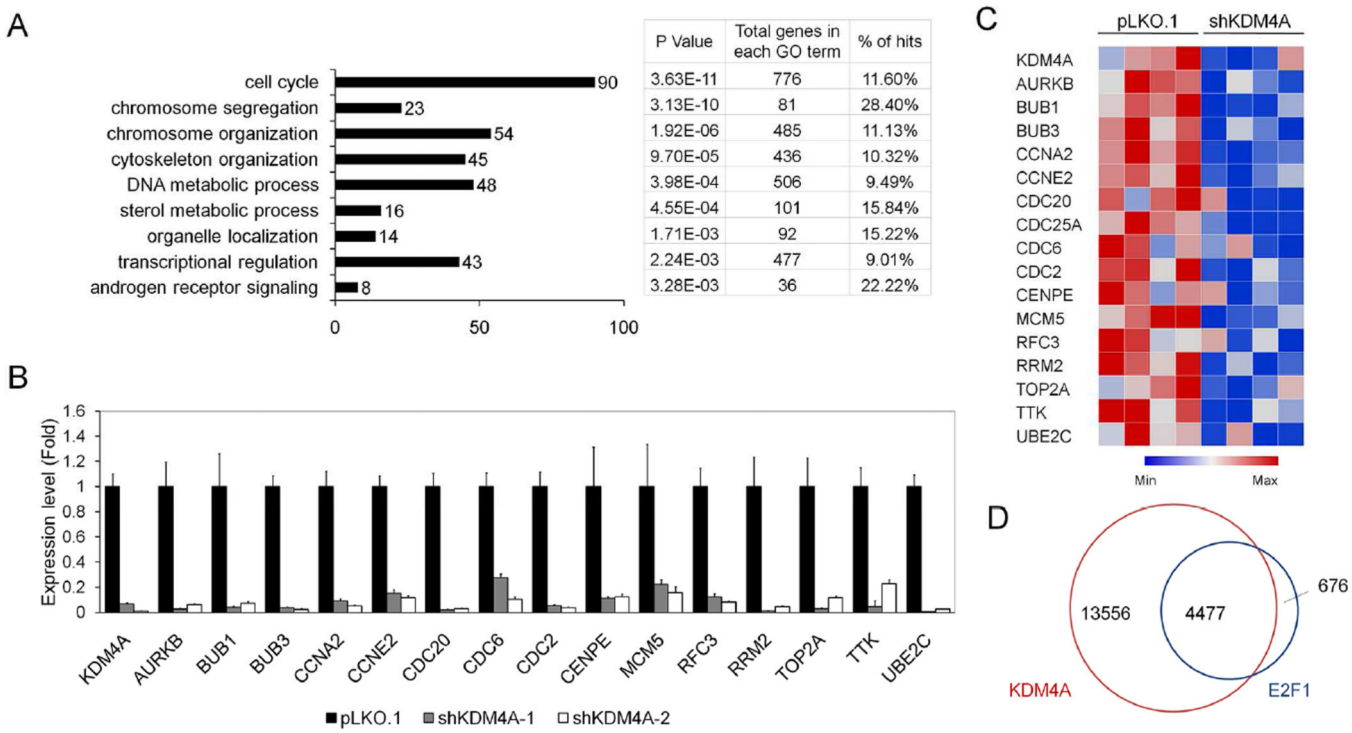

Figure 2.

KDM4A regulates expression of E2F1 target genes. (A) DAVID functional annotation and pathway analysis of the genes that showed two-fold alterations in KDM4A-knockdown LNCaP cells in microarray analysis. GOs that showed statistically strong enrichment of alteration with low P-values are listed. Bar graph and the numbers indicate gene counts of each pathway. % of hits indicates the percentage of genes that are altered in each GO. (B) Gene expression in LNCaP cells transduced with control or shKDM4A for 3 days was detected by qRT-PCR. The data is presented as the average of n= 3 replicates ± SD. The statistics of difference between shKDM4A and pLKO.1 is $p< 0.01$. (C) qRT-PCR analysis of the gene expression in 8 tumors isolated from CWR22Rv1-pLKO.1 and -shKDM4A xenografts. Color scheme indicates Max and Min expression across the 8 tumor specimens. (D) Intersection of published KDM4A (GSM831035) and E2F1 (GSM935366) ChIP-seq binding sites examined in hESC and HeLa cells, respectively.

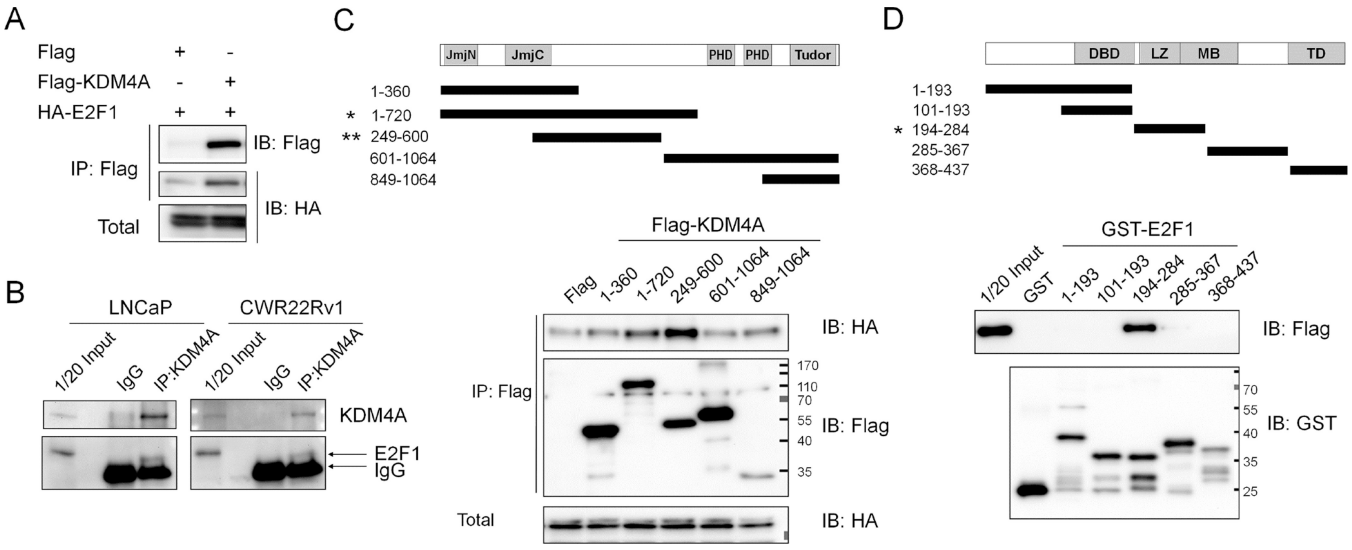

Figure 3.

KDM4A associates with E2F1. (A) Association of ectopically expressed KDM4A with E2F1.293T cells were co-transfected with Flag or Flag-KDM4A and HA-E2F1 followed by IP using anti-Flag antibody. The co-IP'd E2F1 was detected by anti-HA antibody with immunoblotting (IB). (B) Endogenous association of KDM4A and E2F1. LNCaP and CWR22Rv1 cell lysates were used for KDM4A IP, and the co-IP'd E2F1 was detected by anti-E2F1 antibody. Mouse normal IgG was used as negative control. (C) Flag-KDM4A truncated proteins and HA-E2F1 were co-expressed in 293T cells for co-IP as described above. Asterisks indicate positive binding. (D) *In vitro* GST pull-down assay of recombinant GST-E2F1 fragments with purified Flag-KDM4A protein. Asterisks indicate positive binding. DBD, DNA binding domain; LZ, leucine zipper; MB, marked box; TD, transactivation domain.

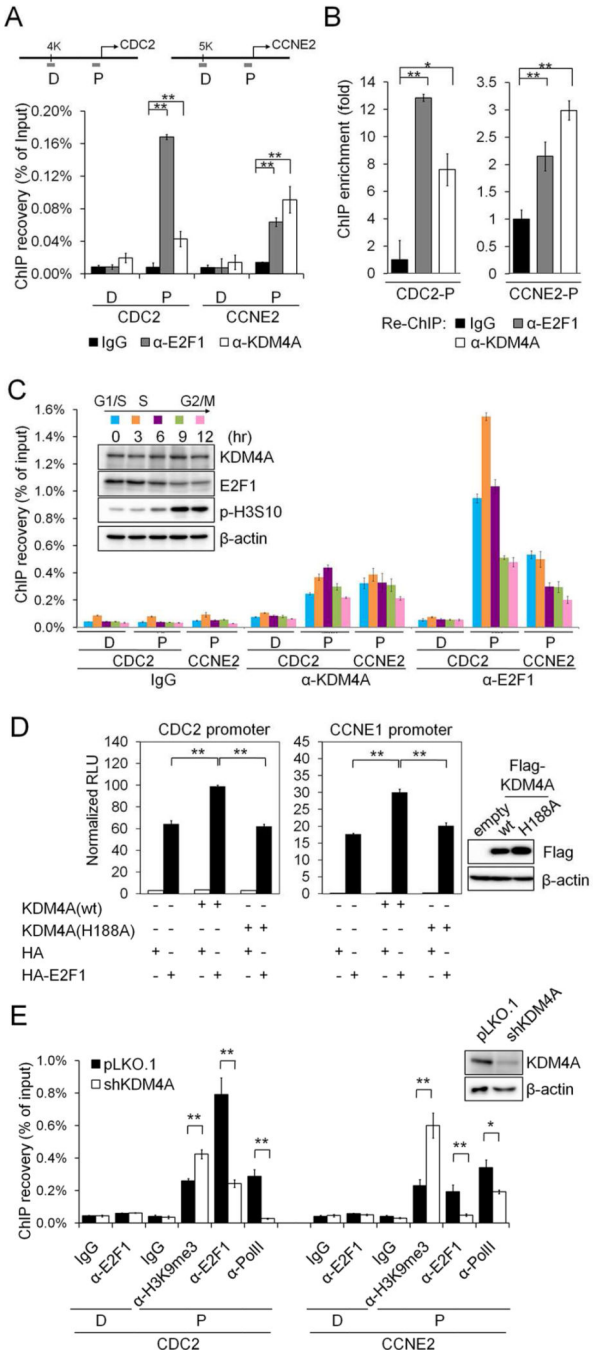

Figure 4.

Chromatin recruitment of KDM4A with E2F1 enhances E2F1 transcriptional activity. (A) ChIP analysis of KDM4A and E2F1 occupancy on CDC2 and CCNE2 promoters in LNCaP cells using IgG, anti-KDM4A or anti-E2F1 antibodies. ChIP DNAs were analyzed by qPCR with primers that amplify genomic regions either proximal (P) or distal (D) to TSS for each gene. (B) ChIP-reChIP assay of KDM4A and E2F1 binding. LNCaP chromatin was used for the first ChIP with anti-KDM4A. The KDM4A bound chromatin was eluted and subjected to reChIP using IgG, anti-E2F1 or anti-KDM4A, followed by qPCR analysis of the target sites.

(C) KDM4A and E2F1 occupancy on the target promoters during cell cycle progression. LNCaP cells were arrested at G1/S transition by double thymidine block and subsequently released to complete medium at 0 hr. Cells at the indicated time points were harvested for KDM4A and E2F1 ChIP assays. The protein levels and phospho-H3S10, indicating the stage of mitosis are shown in the western blots. (D) CDC2 and CCNE1 promoter activities. The CDC2 and CCNE1 promoter-luciferase constructs were co-expressed with empty HA or HA-E2F1, and wild type (wt) or inactive (H188A) KDM4A in PC3 cells. The luciferase activity was measured 48 hours after transfection. (E) Enrichment of E2F1, PolII and H3K9me3 on the target promoters in control and KDM4A-knockdown LNCaP cells. The level of H3K9me3 was normalized by histone H3. The western blot shows KDM4A level. All data are presented as the average of n= 3 replicates ± SD. **:$p<0.01$, *:$p<0.05$.

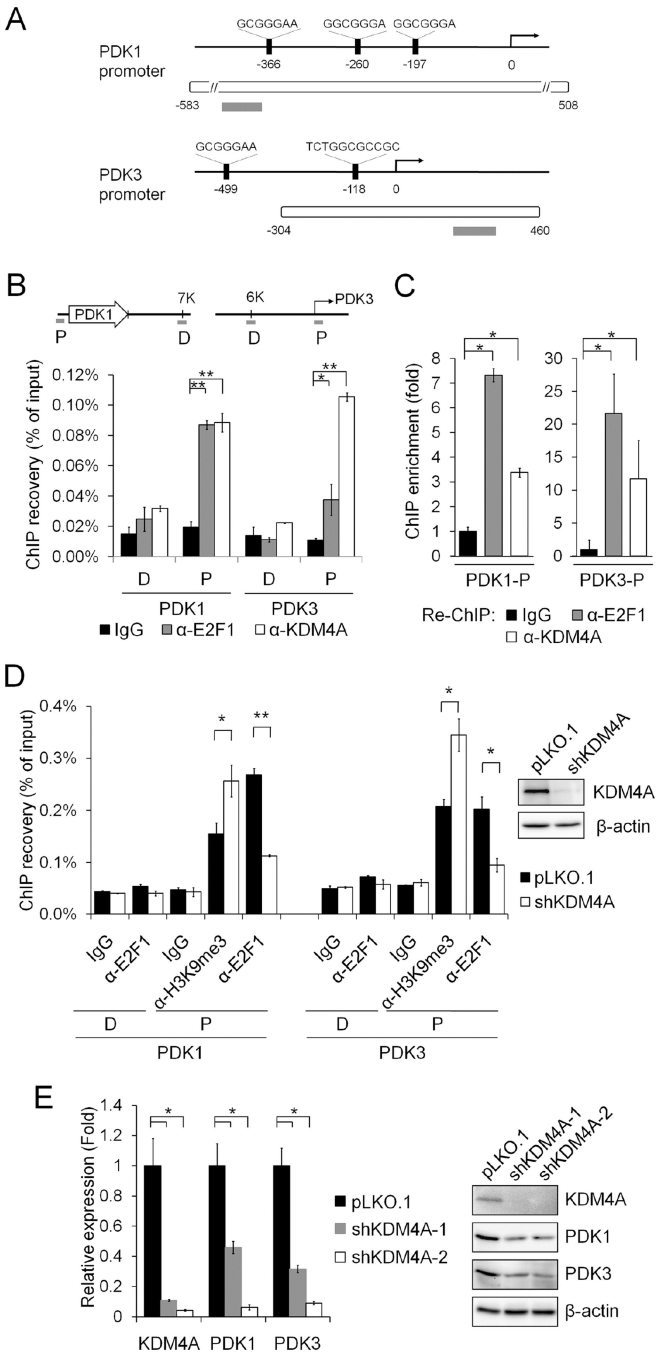

Figure 5.

PDK1 and PDK3 are direct targets of KDM4A and E2F1. (A) Schematic PDK1 and PDK3 promoters. Black bars indicate putative E2F response elements and the consensus sequence. White bars indicate E2F1 binding sites identified in ENCODE ChIP-seq analysis. Grey bars indicate the qPCR amplification sites proximal to the TSS used in this study. (B) ChIP-qPCR analysis of KDM4A and E2F1 occupancy on proximal (P) or distal (D) regions of PDK1 and PDK3 promoters in LNCaP cells. The distal site for PDK1 was designed at the intergenic region downstream of PDK1. (C) ChIP-reChIP assay of KDM4A and E2F1

binding on the PDK1 and PDK3 promoters, as described in Figure 4B. (D) Enrichment of E2F1 and H3K9me3 on PDK1 and PDK3 promoters in control and KDM4A-knockdown LNCaP cells. The H3K9me3 level was quantified as described in Figure 4E. (E) RNA and protein levels of KDM4A, PDK1 and PDK3 in pLKO.1 and shKDM4A cells. LNCaP cells infected for 3 days were harvested for qRT-PCR and western blotting. All data are presented as the average of n= 3 replicates ± SD. **: $p< 0.01$, *:$p< 0.05$.

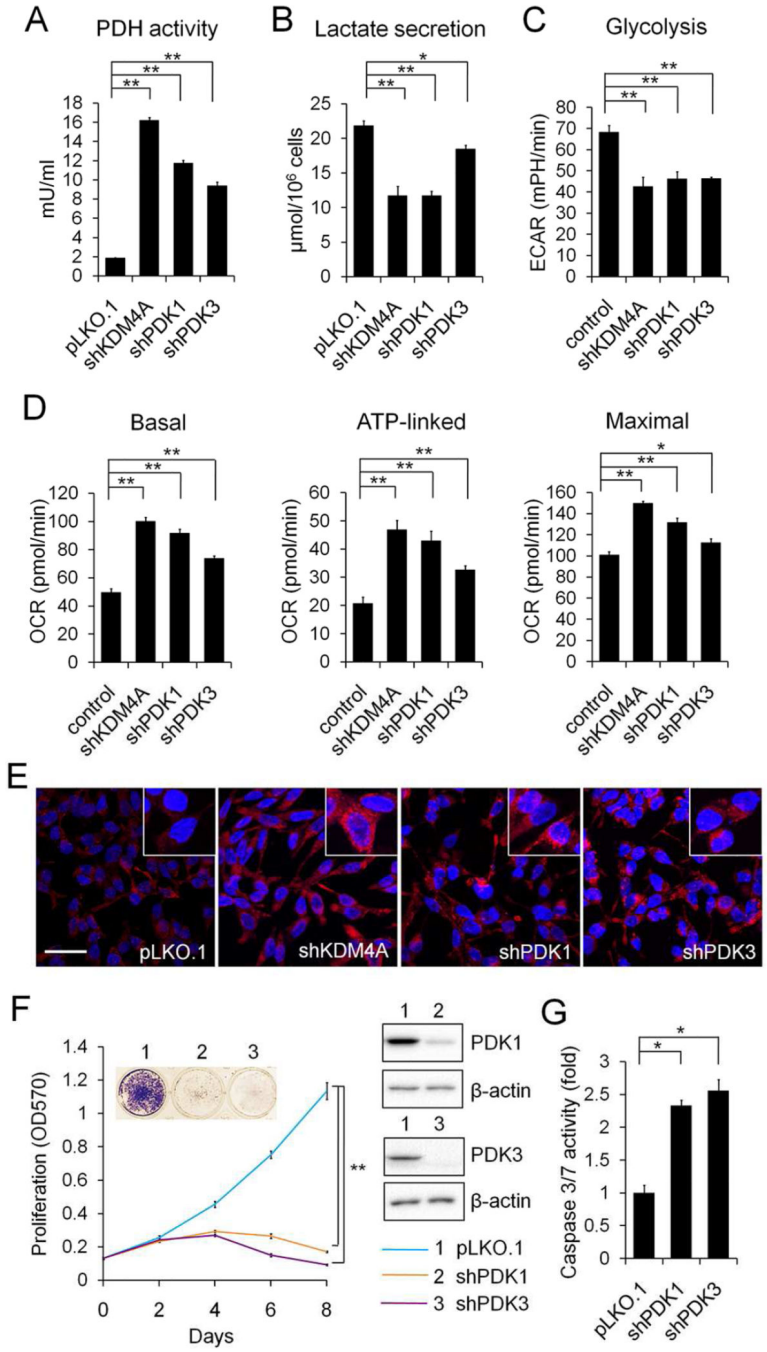

Figure 6.

Knockdown of KDM4A, PDK1 or PDK3 induces mitochondrial metabolism. LNCaP cells were infected by lentivirus carrying pLKO.1, shKDM4A, shPDK1 or shPDK3. 3 days after infection, the cells and cultured media were harvested to measure cellular (A) PDH activity and (B) lactate secretion. The PDH activity was normalized by protein concentration of the cell lysates. (C–D) The cellular ECAR and OCR were measured on day 3 after lentiviral infection. (E) Mitochondrial ROS was detected by MitoSOX fluorescence dye 4 days after transduction. Images from randomly selected fields were taken. Scale bar: 50 μm. (F,G) Cell

growth and caspase 3/7 activity in shPDK1 and shPDK3 cells were examined as described in Figure 1A, 1B and 1D. PDK1 and PDK3 expression is shown in the western blots. All data are presented as the average of n= 3 replicates ± SD. **: $p< 0.01$, *: $p< 0.05$.

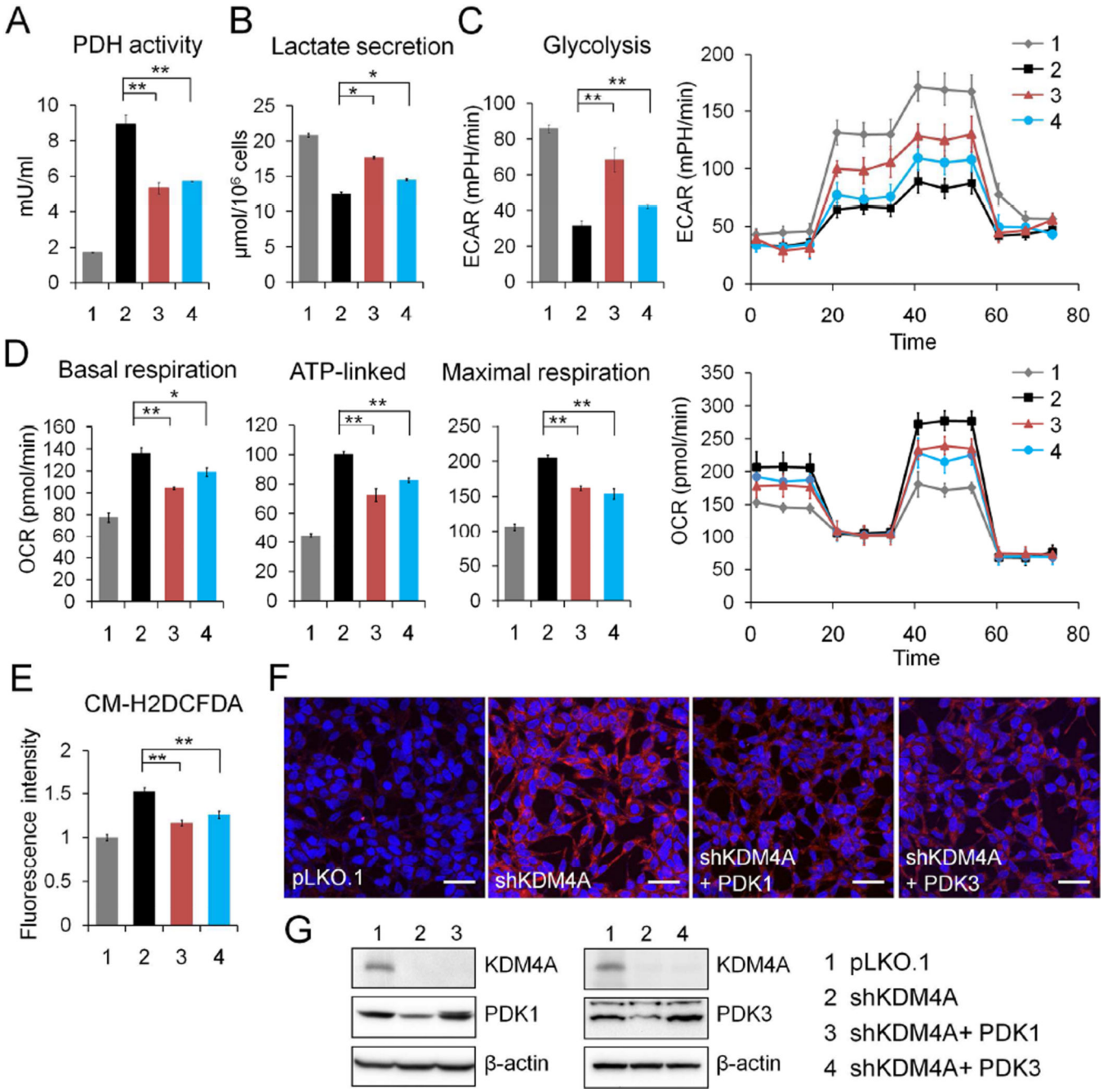

Figure 7.

Ectopic expression of PDK1 and PDK3 rescues the KDM4A metabolic phenotypes. Lentivirus carrying PDK1 or PDK3 overexpression constructs were used to infect LNCaP cells together with the shKDM4A virus. (A) PDH activity, (B) lactate production, (C) ECAR and (D) OCR were measured as described in Figure 6 3 days after infection. (E) Total cellular ROS was labeled by CM-H2DCFDA. (F) Mitochondrial ROS was detected by MitoSOX fluorescence dye as described above. Scale bar: 50 μm. (G) KDM4A, PDK1 and

PDK3 protein levels were examined 3 days after infection. All data are presented as the average of n= 3 replicates ± SD. **: $p < 0.01$, *: $p < 0.05$.